Power Scheduling of Distributed Generators for Economic and Stable Operation of a Microgrid

Seon-Ju Ahn, *Member, IEEE*, Soon-Ryul Nam, *Member, IEEE*, Joon-Ho Choi, *Member, IEEE*, and Seung-Il Moon, *Member, IEEE*

***Abstract*—This paper is concerned with the power dispatch problem of distributed generators (DGs) for optimal operation of a microgrid. The objective is to minimize the fuel cost during the grid-connected operation, while ensuring stable operation after islanding. To achieve this goal, the economic dispatch (ED) problem and related constraints are formulated. The constraints considered in this study are: i) reserve for variation in load demand, ii) reserve for variation in the power outputs of non-dispatchable DGs, iii) flow limits between two adjacent areas, and iv) reserve for the stable islanded operation. The first three constraints, which have been employed in ED problem for conventional power systems, are modified to apply to Microgrids. We also provide a detailed formulation of the constraint for stable islanded operation in accordance with two power-sharing principles: i) fixed droop and ii) adjustable droop. The problem is solved using a modified direct search method, and the effect of the constraints on the operational cost is investigated via numerical simulations.**

***Index Terms*—Distributed generator, economic dispatch, islanded operation, microgrid, smart grid.**

NOMENCLATURE

g	Dispatchable DG unit index.
N_{gen}	Number of dispatchable units.
P_{g}	Power output of dispatchable unit g.
N_{ND}	Number of non-dispatchable units.
k	Non-dispatchable DG unit index.
P_{NDk}	Power output of non-dispatchable unit k.
$F_{\mathrm{g}}(\cdot)$	Cost function of unit g.
$P_{\mathrm{g}}^{\max}$	Maximum generation limit of unit g.
$P_{\mathrm{g}}^{\min}$	Minimum generation limit of unit g.
d	Load index.
N_{load}	Number of loads.
LD_{d}	Power demand of load d.
P_{Main}	Power injected by the main grid.
P_{Ai}	Sum of power outputs of DGs in area i.
LD_{Ai}	Sum of load demands in area i.
$FL_{\mathrm{i\_j}}$	Power flow from area i to area j.
$FL_{\mathrm{i\_j}}^{\max}$	Flow limit from area i to area j.
$P_{\mathrm{Ai}}^{\min}$	Sum of the minimum limits of the units in area i.
$P_{\mathrm{Ai}}^{\max}$	Sum of the maximum limits of the units in area i.

Manuscript received November 28, 2012; accepted December 09, 2012. This study was financially supported by Chonnam National University, 2011 (Research Program 2011-0611). Paper no. TSG-00827-2012.

S.-J. Ahn and J.-H. Choi are with the Department of Electrical Engineering, Chonnam National University, Gwangju 500-757, Korea (e-mail: sjahn@jnu.ac.kr; joono@chonnam.ac.kr).

S.-R. Nam is with the Department of Electrical Engineering, Myongji University, Yongin 449-728, Korea (e-mail: ptsouth@mju.ac.kr).

S.-I. Moon is with the School of Electrical Engineering, Seoul National University, Seoul 151-742, Korea (e-mail: moonsi@plaza.snu.ac.kr).

Color versions of one or more of the figures in this paper are available online at http://ieeexplore.ieee.org.

Digital Object Identifier 10.1109/TSG.2012.2233773

I. INTRODUCTION

ELECTRIC power systems have been undergoing profound changes in response to various needs, such as environmental compliance, energy conservation, better grid reliability, improved operational efficiency, and customer service [1]. "Smart grid," "intelligent grid," and "next-generation grid" are the names applied to the power grid of the future, in which the electrical infrastructures and intelligent information networks will be integrated in order to satisfy the aforementioned needs [1]–[4]. In the meantime, the increasing use of distributed energy resources (DERs), including intermittent renewable sources, will pose many challenges for the future grid, especially with regard to the distribution system [1]. In order to solve the interconnection problems of individual distributed generators (DGs), the concept of a microgrid has been proposed [5]–[7]. A microgrid is a low- or medium-voltage distribution network, comprising various DGs, storage devices, and controllable loads, which can be operated in either the grid-connected or islanded mode [5], [6]. To date, there have been numerous research projects on the design, control, and operation of microgrids throughout the world, such as the CERTS microgrid in USA [6], [7], the MICROGRID project of Europe [8], and the new energy integration test project carried out by NEDO in Japan [9].

In [8] and [10]–[13], a central controller and an energy management system (EMS) were proposed as a means of deriving the greatest benefit from the operation of a microgrid, and increasing the efficiency of DG usage. The principal functions of a microgrid EMS are to provide power and voltage set points for each DG controller, to meet the heat and electrical loads, to satisfy the operational contracts with the main system, to minimize emissions and losses, and to provide logic and control for fast and stable islanding during grid faults. To accomplish these functions, a microgrid EMS uses a variety of information, such as local electrical and heat demands, weather, the price of electric power, fuel cost, and power quality requirements [6], [11].

Among the above functions, this paper focuses on the problem of determining the power references of DGs for the optimal operation of a microgrid. The optimization of a microgrid has important differences from the case of a large power system and its conventional economic dispatch (ED) problem [13]. One of the most important differences is the necessity for stable mode transition from a grid-connected to the islanded operation in case of grid faults. Therefore, we propose the formulations of the ED problem for microgrids and its related constraints, which yield the fuel cost minimization during the grid-connected operation while ensuring stable operation after islanding.

The remainder of this paper is divided into five sections. Section II introduces several issues regarding the power control of DGs in a microgrid. In Section III, the economic dispatch problem and related constraints are formulated for a microgrid. Section IV presents the formulation of the constraint for the stable islanded operation in accordance with the power-sharing principle between the DGs. Section V discusses the numerical simulation results which are utilized to investigate the effect of each constraint on the operational cost. Finally, Section VI contains some concluding remarks.

II. Technical Issues Related to Microgrid ED

A. Active Power and Frequency Control in a Microgrid

Before developing the formulation of the ED problem for a microgrid, we will briefly discuss some technical issues related to the active power and frequency control of DGs: 1) the power-control mode, 2) the power-sharing principle among DGs during microgrid islanding, and 3) the controllability of energy sources.

1) Power-Control Mode: The power output of a DG can be controlled by one of two different modes: unit output power control (UPC) or feeder flow control (FFC) [7]. A UPC-mode DG generates constant active power according to the power reference, while the output of an FFC-mode DG is controlled so that the active power flow in the feeder remains constant. In this study, the power output reference for a UPC-mode DG and the feeder flow reference for an FFC-mode DG are determined by solving the ED problem regarding the optimal operation of a microgrid.

2) Power-Sharing Principle During Microgrid Islanding: When a microgrid is disconnected from the main grid, DGs must take the place of the main grid in matching the power demand. In many studies, power versus frequency $(P - f)$ droop control has been adopted in order to ensure that the power demand is dynamically balanced by the DGs [5]–[8]. Conventionally, the droop constant of a DG is considered to be a fixed parameter, determined so that the load demand is shared among DGs in proportion to their rated capacities. In [14] and [15], a new power-sharing principle is proposed in which the droop constants are periodically modified according to the operating points of the DG units. With this method, the DGs share power according to their operational reserves, rather than their capacities. We refer to the former techniques as *fixed droop* and the latter techniques as *adjustable droop*, and formulate the constraint related to the islanded operation of a microgrid in accordance with the power-sharing principle.

3) Controllability of Energy Sources: The emerging generation technologies suitable for microgrid application, together with their typical capacity ranges, are listed in Table I [16]. Since most DGs are interfaced with the grid through an inverter, they have various control capabilities, including power, frequency, and voltage control. However, the power outputs of DGs with renewable energy sources, such as photovoltaic cells and wind turbines, are driven by weather, not by system loads [7]. Therefore, these intermittent sources cannot be used as dispatchable sources. In the ED problem, these sources will be treated as negative loads, and their power outputs will be assumed to be predictable within some range of uncertainty.

TABLE I
Characteristics of Typical DG Energy Sources

Energy source type	Capacity range	Dispatchability
Internal combustion engines	10 kW ~ 10 MW	O
Small size combustion turbines	0.5 ~ 50 MW	O
Microturbines	20 ~ 500 kW	O
Fuel cells	1 kW ~ 10 MW	O
Photovoltaic systems	5 W ~ 5 MW	X
Wind turbines	30 W ~ 10 MW	X

B. Constraints Associated With Microgrid Operation

As Fig. 1 indicates, the microgrid configuration considered in this study is a multiple-FFC configuration, which is most suitable for a microgrid in which none of the DGs are dominant [17], [18]. We assume that the variation of loads and the power outputs of non-dispatchable DGs in each control area are compensated by the dispatchable DGs in the same area. To accomplish this, the first DG in each area operates in the FFC mode, while the others operate in the UPC mode, as shown in Fig. 1(b). With this configuration, any variation within an area can be compensated by the FFC-mode DG, and the flow between two adjacent areas remains unchanged over a predetermined time period [17]–[20]. This property is advantageous to system operators, since microgrids can be thought of as controllable subsystems.

The basic ED problem is extended to include the additional constraints related to the operation of a microgrid. The constraints considered in this study are as follows:

i) Reserve for variation in load demand
ii) Reserve for variation in the power outputs of non-dispatchable DGs
iii) Flow limits between two adjacent areas
iv) Reserve for the stable islanded operation.

Since the first three constraints have already been adopted as part of the ED problem for conventional power systems, they are simply modified for application to a microgrid. The unique constraint, concerning the reserve for the stable islanded operation, will be discussed in detail in Section IV.

III. ED Problem Formulation for a Microgrid

A. Formulation of the Basic ED Problem

In a power system, the primary objective of the ED is to minimize the total generation cost (F_{T}), while satisfying the power balance and generation limits of the units [21], [22]. This can be formulated as follows:

$$\min F_T = \sum_{g=1}^{N_{gen}} F_g(P_g) \tag{1}$$

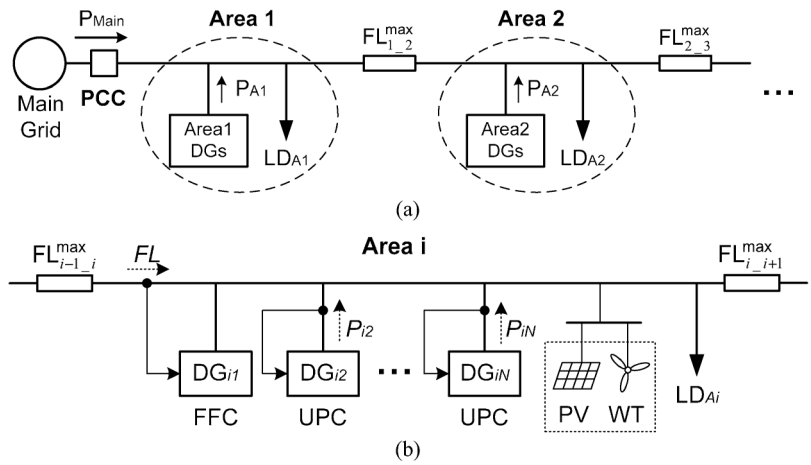

Fig. 1. Microgrid configuration. (a) Configuration of a microgrid with multiple control areas. (b) Configuration of a control area.

subject to

$$\sum_{g=1}^{N_{gen}} P_g = \sum_{d=1}^{N_{load}} LD_d \tag{2}$$

$$P_g^{\min} \le P_g \le P_g^{\max}. \tag{3}$$

B. Modification of the Constraint Formulations

1) Power Balance Constraints: The power balance condition is modified as (4), taking into account the power outputs of the non-dispatchable sources and the power injected by the main grid. The load demand and the power outputs of intermittent sources are assumed to be predicted for every time interval.

$$\sum_{g=1}^{N_{gen}} P_g + P_{Main} = \sum_{d=1}^{N_{load}} LD_d - \sum_{k=1}^{N_{ND}} P_{ND_k} \tag{4}$$

2) Spinning Reserve Requirement Constraints: Normally there are uncertainties involved in predicting load demand and wind velocity and/or irradiance. Moreover, load demand and the power outputs of intermittent sources usually vary continuously. In order to compensate for these variations, and to operate the system stably, additional reserve is necessary. For a microgrid with the proposed configuration, in which all the variations are picked up by the FFC-mode DG in each area, the constraint can be formulated as (5) and (6). The spinning reserve requirement is reflected as a decrease in the maximum limit ($P_{\mathrm{i1}}^{\max}$) and an increase in the minimum limit ($P_{\mathrm{i1}}^{\min}$) of the first DG within each area. In this study, it is assumed that the load demand varies within $r\%$ of the predicted value, and the power outputs of the non-dispatchable sources vary within $u\%$ of the predicted value.

$$P_{i1} \le P_{i1}^{\max} - \left(\frac{r}{100} \cdot \sum_{d \in A_i} LD_d + \frac{u}{100} \cdot \sum_{k \in A_i} P_{ND_k} \right) \tag{5}$$

$$P_{i1} \ge P_{i1}^{\min} + \left(\frac{r}{100} \cdot \sum_{d \in A_i} LD_d + \frac{u}{100} \cdot \sum_{k \in A_i} P_{ND_k} \right) \tag{6}$$

3) Inter-Area Flow Limit Constraints: As Fig. 1(a) indicates, the power flow between two adjacent areas is restricted by the physical limits ($FL^{\max}$). This constraint can be formulated as (7)–(10), assuming that the number of areas in a feeder is n. Note that the power flow from/to the main grid (P_{Main}) is reflected by a decrease/increase in the load on the area nearest the main grid (i.e., area 1), according to (7).

$$P_{A_1} = LD_{A_1} - P_{Main} + FL_{1\_2} \qquad for\ Area_1 \tag{7}$$

$$P_{A_i} = LD_{A_i} + FL_{i\_i+1} - FL_{i-1\_i} \quad for\ Area_i \quad i = 2, \ldots, n-1 \tag{8}$$

$$P_{A_n} = LD_{A_n} - FL_{n-1\_n} \qquad for\ Area_n \tag{9}$$

$$-FL_{i-1\_i}^{\max} \le FL_{i-1\_i} \le FL_{i-1\_i}^{\max} \qquad i = 2, \ldots, n \tag{10}$$

IV. Formulation of the Constraint for the Stable Islanded Operation

When a microgrid is islanded, the DGs will adjust their power outputs according to the power-frequency droop characteristics, in order to compensate for the loss of the main grid. Since the system topology is radial, a power output change from any DG will affect the power flow in the upstream lines. For example, if power is imported from the main grid during the grid-connected operation, the DGs will increase their power outputs, and thus the upward flow in each line will be increased. Accordingly, if the power flow between two areas has remained near its maximum limit during the grid-connected operation, power cannot be transmitted during the transition, and this can make the system unstable.

In [8] and [23], load shedding algorithms have been proposed for stable operation in case of such contingencies. However, in this paper, we assume that the DGs are capable of supplying all loads without curtailment during the islanded operation. For this reason, the DGs should have at least as much reserve as P_{Main} during the grid-connected operation. Furthermore, the inter-area flow limit should also be refined when determining the power output reference of the DGs. The more the flow limits are restricted, the more stable the system will be when islanded. However, such restriction will increase the operational cost during the grid-connected operation. Therefore, we propose a method for determining the optimal values of flow limits that satisfy the above two objectives (i.e., cost minimization during the grid-connected operation and the stable islanded operation). This section presents the formulation of this constraint in accordance with each of the two different power-sharing principles (fixed droop and adjustable droop).

A. Constraint Formulation With Fixed Droop

With this power-sharing principle, each DG will change its power output in proportion to the inverse of the predetermined droop constant (R_{g}). Since the sum of the power output changes should be equal to the magnitude of P_{Main}, the power picked up by a unit g during islanding ($\Delta P_{\mathrm{g}}^{\mathrm{IM}}$) can be calculated from (11).

$$\Delta P_g^{IM} = \frac{\frac{1}{R_g}}{\sum_{j=1}^{N_{gen}} \frac{1}{R_j}} \cdot |P_{Main}| \tag{11}$$

Similarly, the amount of power shared by area i ($\Delta P_{\mathrm{Ai}}^{\mathrm{IM}}$) can be calculated as the sum of the contributions for all the units in area i, as follows.

$$\Delta P_{A_i}^{IM} = \frac{\sum_{g \in A_i} \frac{1}{R_g}}{\sum_{j=1}^{N_{gen}} \frac{1}{R_j}} \cdot |P_{Main}| \tag{12}$$

The constraints can be formulated differently, depending on whether the power is initially imported from or exported to the main grid.

1) Power Initially Exported: When the microgrid supplies power to the main grid during the grid-connected operation (i.e., $P_{\mathrm{Main}} < 0$), the DGs will decrease their power outputs during the transition. Accordingly, all DGs should have additional down spinning reserve, and this is reflected by an increase in the minimum limit of the unit, as follows.

$$P_g^{\min} + \Delta P_g^{IM} \le P_g \le P_g^{\max} \tag{13}$$

Since the DGs decrease their power outputs, the downward flow between areas will increase during the transition. Therefore, for the stable islanded operation without violating the physical inter-area flow limits, the downward flow should be maintained at an appropriate level below the limit during the grid-connected operation. The amount of additional flow from area $(i-1)$ to area i is the sum of the power shared by the DGs in area i and the areas downstream from it. Accordingly, the downward flow limit should be decreased by the amount of additional flow, whereas the upward flow limit remains unchanged.

$$-FL_{i-1\_i}^{\max} \le FL_{i-1\_i} \le \left(FL_{i-1\_i}^{\max} - \sum_{a=i}^{n} \Delta P_{A_a}^{IM} \right) \quad i = 2, \ldots, n \tag{14}$$

2) Power Initially Imported: If power is imported from the main grid during the grid-connected operation (i.e., $P_{\mathrm{Main}} > 0$), the DGs will increase their power outputs when the microgrid is disconnected from the main grid. Contrary to the former case, all DGs should have additional up spinning reserve, and the upward flow will be increased in the inter-area lines. Therefore, the maximum limits of the DGs and the upward flow limit should be decreased in accordance with (15) and (16), respectively.

$$P_g^{\min} \le P_g \le P_g^{\max} - \Delta P_g^{IM} \tag{15}$$

$$-\left(FL_{i-1\_i}^{\max} - \sum_{a=i}^{n} \Delta P_{A_a}^{IM} \right) \le FL_{i-1\_i} \le FL_{i-1\_i}^{\max} \quad i = 2, \ldots, n \tag{16}$$

B. Constraint Formulation With Adjustable Droop

When fixed droop is adopted, the contribution of each DG to the reserve is determined before solving the ED problem, and thus the output limit of a unit is modified according to (13) or (15). However, when adjustable droop is applied, the power output reference for each DG is determined optimally, and the contribution to the reserve is then determined according to its operational margin [14], [15]. Hence, the output limits of the DGs do not need to be modified. The inter-area flow limits, on the other hand, should be refined as in the case of fixed droop.

1) Power Initially Exported: As was noted in the fixed droop case, the DGs will decrease their power outputs in order to compensate for the loss of the main grid. If we assume that the output of unit g is P_{g}, the operational margin of this unit is $P_{\mathrm{g}} - P_{\mathrm{g}}^{\min}$. Therefore, the power shared by unit g during the transition ($\Delta P_{\mathrm{g}}^{\mathrm{IM}}$) can be calculated as follows.

$$\Delta P_g^{IM} = \frac{P_g - P_g^{\min}}{\sum_{j=1}^{N_{gen}} \left(P_j - P_j^{\min} \right)} \cdot |P_{Main}| \tag{17}$$

As in the fixed droop case, the amount of power shared by area i (ΔP_{Ai}^{IM}) can be calculated as the sum of the contributions regarding all units in area i.

$$\Delta P_{A_i}^{IM} = \frac{P_{A_i} - P_{A_i}^{\min}}{\sum_{j=1}^{N_{gen}} \left(P_j - P_j^{\min} \right)} \cdot |P_{Main}| \tag{18}$$

The downward flow limits should be decreased in a manner similar to (14). However, in this case, since the power shared by each unit is unknown until the ED problem is solved, the decreased value for the downward flow limits cannot be calculated directly as in the case of the fixed droop.

The downward power flow from area $(i-1)$ to area i during the grid-connected operation is the sum of the differences between the load demands and power outputs of area i and the areas downstream from it.

$$FL_{i-1\_i} = \sum_{a=i}^{n} (LD_{A_a} - P_{A_a}) \tag{19}$$

The additional flow in the line between area $(i-1)$ and area i during the transition ($\Delta FL_{\mathrm{i-1\_i}}$) can be calculated as follows.

$$\Delta FL_{i-1\_i} = \sum_{a=i}^{n} \Delta P_{A_a}^{IM} = \frac{\sum_{a=i}^{n} P_{A_a} - \sum_{a=i}^{n} P_{A_a}^{\min}}{\sum_{g=1}^{N_{gen}} \left(P_g - P_g^{\min} \right)} \cdot |P_{Main}| \tag{20}$$

Using the power balance equation given in (4), the denominator of the right-hand side of (20) can be rewritten as in (21). For the sake of simplicity, it is assumed that the power outputs of the non-dispatchable DGs are included in the load as negative values.

$$\sum_{g=1}^{N_{gen}} \left(P_g - P_g^{\min} \right) = \sum_{d=1}^{N_{load}} LD_d + |P_{Main}| - \sum_{g=1}^{N_{gen}} P_g^{\min} \tag{21}$$

By substituting (19) and (20) into the right-hand side of (14), we can obtain (22).

$$\sum_{a=i}^{n} LD_{A_a} - \sum_{a=i}^{n} P_{A_a} \le FL_{i-1\_i}^{\max} - \frac{\sum_{a=i}^{n} P_{A_a} - \sum_{a=i}^{n} P_{A_a}^{\min}}{\sum_{d=1}^{N_{load}} LD_d + |P_{Main}| - \sum_{g=1}^{N_{gen}} P_g^{\min}} \cdot |P_{Main}| \quad (22)$$

Since all the variables, except the power outputs of the DGs, are known, (22) can be rewritten in the form of the equation at the bottom of the page. Combining (19) and (23), the modified downward flow limit can be determined from (24).

$$FL_{i-1\_i} \le FL_{i-1\_i}^{\max} - |P_{Main}| \cdot \left(\frac{\sum_{a=i}^{n} LD_{A_a} - \sum_{a=i}^{n} P_{A_a}^{\min} - FL_{i-1\_i}^{\max}}{\sum_{d=1}^{N_{load}} LD_d - \sum_{g=1}^{N_{gen}} P_g^{\min}} \right) \quad (24)$$

2) Power Initially Imported: In this case, the DGs will increase their power outputs in order to compensate for the loss of the main grid, and thus the upward flow limit should be modified. Since the operational margin of unit g in this case is $P_{\mathrm{g}}^{\max} - P_{\mathrm{g}}$, the amount of power shared by area i ($\Delta P_{\mathrm{Ai}}^{\mathrm{IM}}$) can be calculated as follows.

$$\Delta P_{A_i}^{IM} = \frac{P_{A_i}^{\max} - P_{A_i}}{\sum_{g=1}^{N_{gen}} \left(P_g^{\max} - P_g \right)} \cdot |P_{Main}| \quad (25)$$

Since the power balance equation for this case is as in (26), the left-hand side of (16) can be written as (27), using a procedure similar to that used in the previous case.

$$\sum_{g=1}^{N_{gen}} P_g + |P_{Main}| = \sum_{d=1}^{N_{load}} LD_d \quad (26)$$

$$- \left(FL_{i-1\_i}^{\max} - \frac{\sum_{a=i}^{n} P_{A_a}^{\max} - \sum_{a=i}^{n} P_{A_a}}{\sum_{g=1}^{N_{gen}} P_g^{\max} - \sum_{d=1}^{N_{load}} LD_d + |P_{Main}|} \cdot |P_{Main}| \right) \le \sum_{a=i}^{n} LD_{A_a} - \sum_{a=i}^{n} P_{A_a} \quad (27)$$

Finally, the upward flow limit can be calculated as follows.

$$- \left(FL_{i-1\_i}^{\max} - |P_{Main}| \cdot \frac{\sum_{a=i}^{n} P_{A_a}^{\max} - \sum_{a=i}^{n} LD_{A_a} - FL_{i-1\_i}^{\max}}{\sum_{g=1}^{N_{gen}} P_g^{\max} - \sum_{d=1}^{N_{load}} LD_d} \right) \le FL_{i-1\_i} \quad (28)$$

Note that all the variables in (24) and (28) can be calculated from system data, and hence the optimal values of inter-area flow limits can be determined before solving the ED problem.

V. Numerical Simulations and Results

A. Test System Description and Solution Method

We developed system data to test the ED problem for microgrids, since a suitable benchmark system seems to be currently unavailable. In [24], a mathematical formulation for the fuel cost function of a PEM fuel cell is introduced, in which the cost is a function of the generated power (P_{g}), efficiency (η_{g}), and fuel price (C_{g}), as given in (29). The efficiency curve of a fuel cell is determined in [25] as a function of the part-load ratio (PLR, ratio of generated power to maximum power capacity), and the curve is approximated by a fifth-order polynomial, as in (30). For other DG sources, such as microturbines and gas turbines, the efficiency is also reduced at part-load conditions, in comparison to the full-load condition [16]. As with fuel cells, the PLR-efficiency curves of these sources can be approximated by equations of the form given in (30).

$$F_g(P_g) = C_g \cdot \frac{P_g}{\eta_g(PLR)} \quad (29)$$

$$\eta_g(PLR) = e_{1g} + e_{2g} PLR + e_{3g} PLR^2 + e_{4g} PLR^3 + e_{5g} PLR^4 + e_{6g} PLR^5 \quad (30)$$

Firstly, mathematical expressions for the efficiency curves of the DGs with varying source types and/or part-load performances are obtained. The results are listed in Table IV of the Appendix. The fuel cost curve for each DG is then plotted in terms of the generated power, using (29). In this study, the fuel price C_{g} is assumed to be \$0.05/kWh for all DGs, which is equivalent to \$15/MBTU for natural gas [26]. Finally, a cost function, which approximates the curve, is derived for each DG, in the form given by (31). We employ the second-order polynomial as approximating functions, even though they are not completely matched to the curves, since the objective of this paper is to analyze the effects of various constraints on fuel cost, rather than to develop a solution technique for ED problems with complicated cost functions.

$$F_g(P_g) = a_g + b_g P_g + c_g P_g^2 \quad (31)$$

$$- \sum_{a=i}^{n} P_{A_a} \le \frac{\left(\sum_{d=1}^{N_{load}} LD_d - \sum_{g=1}^{N_{gen}} P_g^{\min} + |P_{Main}| \right) \cdot \left(FL_{i-1\_i}^{\max} - \sum_{a=i}^{n} LD_{A_a} \right) + \sum_{a=i}^{n} P_{A_a}^{\min} \cdot |P_{Main}|}{\sum_{d=1}^{N_{load}} LD_d - \sum_{g=1}^{N_{gen}} P_g^{\min}} \quad (23)$$

TABLE II
COST DATA FOR A 15 UNIT TEST SYSTEM

Area	DG	Mode	Cost data			Output limit(kW)	
			a_g	b_g	c_g	P^{max}	P^{min}
Area1	G1	FFC	14.526	0.1032	0.0001	300	35
	G2	UPC	5.0797	0.0792	0.0005	100	20
	G3	UPC	8.7657	0.0656	0.0004	150	30
	G4	UPC	0.8505	0.0689	0.0009	80	10
	G5	UPC	2.0491	0.0301	0.0011	100	20
Area2	G6	FFC	8.5957	0.0346	0.0002	250	60
	G7	UPC	0.8505	0.0689	0.0009	80	10
	G8	UPC	5.0797	0.0792	0.0005	100	20
	G9	UPC	3.4047	0.0134	0.0009	120	30
	G10	UPC	3.4047	0.0134	0.0009	120	30
Area3	G11	FFC	14.526	0.1032	0.0001	300	35
	G12	UPC	5.4976	0.1164	0.0002	150	20
	G13	UPC	5.4976	0.1164	0.0002	150	20
	G14	UPC	1.0171	0.0486	0.0013	75	10
	G15	UPC	3.5442	0.1189	0.0003	100	10
Total						2175	360

TABLE III
DAILY LOAD PATTERN OF THE TEST SYSTEM

Hour	Load (kW)	Hour	Load (kW)
1 ~ 4	1,250	13 ~ 16	1,350
5 ~ 8	1,100	17 ~ 20	1,500
9 ~ 12	1,200	21 ~ 24	1,400

A test system comprising three control areas is utilized for the analysis. We assume that five DGs are installed in each area; the cost data of the DGs and the daily load demands are summarized in Tables II and III, respectively. We also assume that the load demands in Table III include the effects of non-dispatchable DGs, for simplicity. Since the effect of each constraint on the cost varies according to the load distribution, we tested two cases in regards to each condition.

Case 1) Load distribution factor of each area = 0.35 : 0.25 : 0.40

Case 2) Load distribution factor of each area = 0.30 : 0.35 : 0.35

Various mathematical approaches and optimization techniques have been developed for solving ED problems. Chen proposed a direct search method (DSM) for and ED problem with transmission constraints [27], and applied it to ED problems with various types of constraints, such as wind-thermal coordination dispatch and generation-reserve dispatch [28], [29]. In this study, the DSM is applied (with some modifications) in order to solve the ED problem for microgrids, since it offers these definite advantages: i) the algorithm is straightforward and easy to implement, and ii) various inequality and equality constraints can be included. A multi-level convergence strategy, proposed in [27], is also used to improve the performance of the DSM.

B. Test 1: Inter-Area Flow Limit and Load Variation

The first simulation was designed to investigate the effect of the inter-area flow limit and the load variation on generation cost. To accomplish this, the total fuel cost was calculated under various conditions of load distribution, reserve requirement, and inter-area flow limit. The amount of power injected by the main grid, P_{Main}, was assumed to be 0 in this test. The daily fuel costs in terms of the different conditions for the two cases are summarized in Fig. 2.

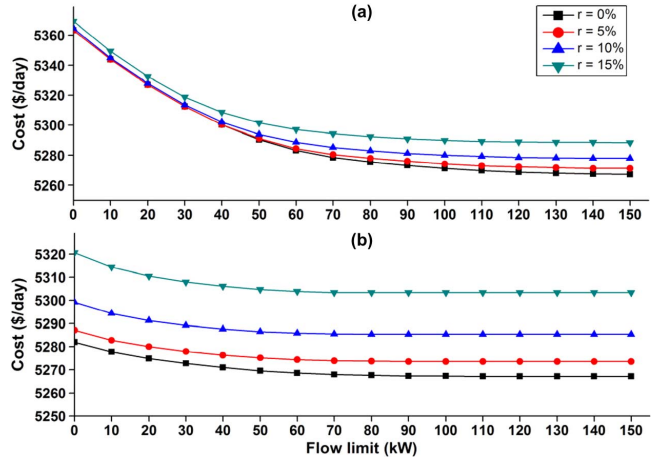

Fig. 2. Effects of inter-area flow limit and load variation reserve. (a) Results for Case 1. (b) Results for Case 2.

The effects of both factors on cost can be summarized as follows. Generation cost increased as the inter-area flow limit became smaller, and this occurred because units with higher incremental cost should increase their outputs as the flow limit decreases. In the test system, the DGs in area 2 had relatively lower incremental cost, but the load level of this area in Case 1 was only 25% of the total demand. Therefore, in order to reduce the total generation cost, the DGs in area 2 should produce more power than the local load demand, and transfer the surplus power to other areas. For example, at a system load of 1500 kW, approximately 22 kW and 118 kW of power were transferred from area 2 to areas 1 and 3, respectively, when the inter-area flow was not limited. However, as the inter-area flow limit decreases, the power transferred from area 2 is restricted, and the units in areas 1 and 3 with higher incremental cost should increase their outputs, which also increases the total generation cost.

We can also see that the cost showed a tendency to increase with the reserve requirement regarding load variation. The power output for the FFC-DGs in each area should be restricted in order to compensate for load variation, in accordance with (5) and (6). Since the incremental costs of the FFC DGs were relatively lower, an increase in the reserve requirement resulted in higher generation cost. Another observation from Fig. 2 is that the effect of the inter-area flow limit was dominant in Case 1, while the effect of load variation reserve was critical in Case 2.

C. Test 2: Reserve for the Stable Islanded Operation

The effect of the reserve for the stable islanded operation was investigated by simulation under various load levels and P_{Main}. We tested the following three conditions with differing load distributions and/or $FL^{\max}$ values, and P_{Main} was varied from -100 to 100 kW in 10 kW steps for each condition.

Condition 1) Load distribution of Case 1 and $FL^{\max} = 40$ kW

Condition 2) Load distribution of Case 2 and $FL^{\max} = 40$ kW

Condition 3) Load distribution of Case 1 and $FL^{\max} = 80$ kW.

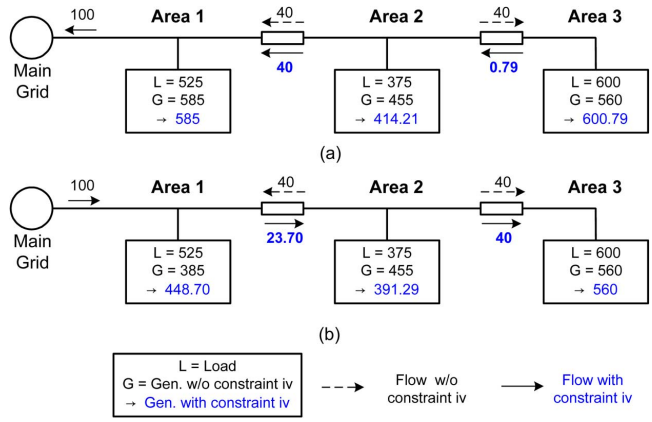

Fig. 3. Sampled result for Condition 1 at load demand $= 1500$ kW. (a) 100 kW is exported. (b) 100 kW is imported.

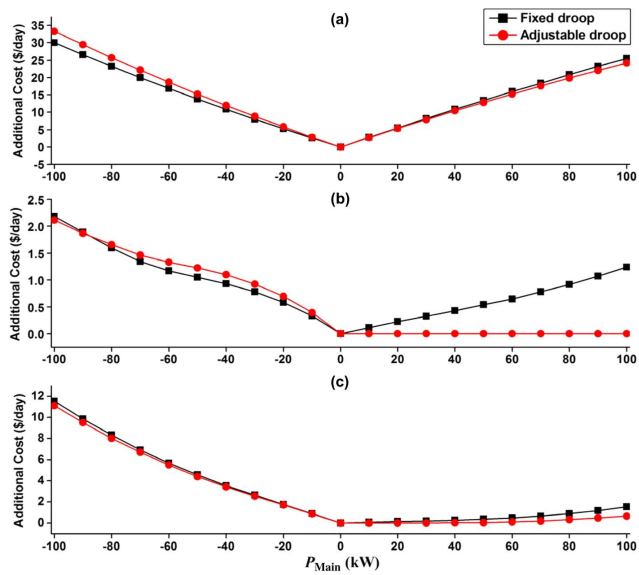

Fig. 4. Additional cost due to the reserve for the stable islanded operation. (a) Results for condition 1. (b) Results for condition 2. (c) Results for condition 3.

Figs. 3(a) and (b) show sampled results for Condition 1 at a 1,500-kW load demand, with $P_{\mathrm{Main}} = -100$ and 100, respectively. We can see that 40 kW of power would have been transferred from area 2 to areas 1 and 3, respectively, in both cases (as indicated by the dashed arrows) if the constraint had not been taken into account. The solutions were altered as follows, considering the reserve for the stable islanded operation. For exported power, the downward flow from area 2 to area 3 was limited to -0.79 kW, where the minus sign signifies that the power was to be transferred from area 3 to area 2. In this case, we can set the flow references of the FFC-DGs in each area at -100, -40, and -0.79, respectively. On the other hand, for imported power, the upward flow from area 2 to area 1 was restricted to -23.70 kW (i.e., actual power transfer from area 1 to area 2), as shown in Fig. 3(b). In both cases, the modified flow limit may increase the operational cost, since the lower-cost DGs in area 2 should decrease their power outputs.

In Fig. 4, the additional cost due to this limit is plotted in terms of P_{Main} for the three conditions. Generally speaking, the additional cost increases as the magnitude of P_{Main} increases, and the following detailed observations can be made. Firstly, the effect of this constraint was more overriding for the load distribution of Case 1 [compare Figs. 4(a) and (b)], and this is because the change in $FL^{\max}$ is not an important factor in the load distribution of Case 2, as discussed in Section V-B. Secondly, if the load distributions were identical, the effect of the constraint would be reduced as $FL^{\max}$ increases [compare Figs. 4(a) and (c)]. Finally, in all cases, the additional cost was less than 0.7% of the total fuel cost, and in some instances, such as power imported in Condition 2 with adjustable droop [denoted by the circle-dotted line of Fig. 4(b)], there was no additional cost increase because of this constraint.

VI. Conclusion

The economic dispatch problem was formulated in accordance with various constraints related to the operation of a microgrid. Some constraints were formulated by modifying existing constraints to fit the configuration of a microgrid. We proposed an additional constraint to ensure the stable islanded operation of a microgrid, and provided a detailed formulation according to the power-sharing principle regarding the DGs. A test system with 15 DG units was developed for numerical simulations, taking into account the source type and part-load performance of each DG. We then investigated the effect of various parameters (including reserve requirement for the load variation, flow limit, load distribution pattern, and the power injected by the main grid) on the cost. Although the cost increased by up to 0.7%, a microgrid could be operated economically during the grid-connected mode, and soundly during the islanded mode, using the modified dispatch solution, which takes into account the additional constraint.

Appendix

The efficiency coefficients of the DGs used in the simulation, in the form given by (30), are listed in Table IV

TABLE IV
Approximated Part-Load Efficiency Data for the DGs

DG		Unit efficiency data						Output limit	
		e_{1g}	e_{2g}	e_{3g}	e_{4g}	e_{5g}	e_{6g}	P^{max}	P^{min}
Area1	1	0.0607	0.5612	-0.4043	-0.4623	0.9022	-0.3912	300	35
	2	0.0636	0.9291	-2.3309	3.4601	-2.5667	0.7247	100	20
	3	0.071	0.5177	-0.4007	-0.0287	0.2003	-0.0795	150	30
	4	0.3747	0.4623	-2.0704	3.6503	-2.9996	0.9033	80	10
	5	0.0883	0.8003	-2.0221	3.0601	-2.3549	0.6985	100	15
Area2	6	0.0607	0.5612	-0.4043	-0.4623	0.9022	-0.3912	300	35
	7	0.0913	0.4694	-0.1085	-1.0011	1.3561	-0.5372	150	20
	8	0.3747	0.4623	-2.0704	3.6503	-2.9996	0.9033	80	10
	9	0.0636	0.9291	-2.3309	3.4601	-2.5667	0.7247	100	20
	10	0.3717	0.0608	0.5602	-2.1454	2.4131	-0.9356	120	30
Area3	11	-0.0822	2.969	-7.9065	10.936	-7.6061	2.0994	200	60
	12	0.3717	0.0608	0.5602	-2.1454	2.4131	-0.9356	120	30
	13	0.0913	0.4694	-0.1085	-1.0011	1.3561	-0.5372	150	20
	14	0.3547	0.5367	-1.7736	2.3437	-1.5412	0.3854	75	10
	15	0.3547	0.5367	-1.7736	2.3437	-1.5412	0.3854	75	10
Total								2100	350

References

[1] A. Ipakchi and F. Albuyeh, "Grid of the future," *IEEE Power Energy Mag.*, vol. 7, no. 2, pp. 52–62, Mar. 2009.

[2] The US Department of Energy (DOE), "The smart grid: An introduction," [Online]. Available: http://www.oe.energy.gov/DocumentsandMedia/DOE_SG_Book_Single_Pages(1).pdf
[3] J. Giri, D. Sun, and R. Avila-Rosales, "Wanted: A more intelligent grid," *IEEE Power Energy Mag.*, vol. 7, no. 2, pp. 34–40, Mar. 2009.
[4] J. D. Mcdonald, "The next-generation grid," *IEEE Power Energy Mag.*, vol. 7, no. 2, pp. 26–94, Mar. 2009.
[5] H. Jiayi, J. Chuanwen, and X. Rong, "A review on distributed energy resources and microgrid," *Renew. Sustain. Energy Rev.*, vol. 12, pp. 2472–2483, 2008.
[6] P. Paolo and R. H. Lasseter, "Microgrid: A conceptual solution," in *Proc. Power Electron. Specialists Conf.*, Jun. 2004, vol. 6, pp. 4285–4290.
[7] R. H. Lasseter, "Control and design of microgrid components," PSERC Final Project Reports [Online]. Available: http://www.pserc.org/cgi-pserc/getbig/publicatio/reports/2006report/lasseter_microgridcontrol_final_project_report.pdf
[8] European Research Project MicroGrids [Online]. Available: http://microgrids.power.ece.ntua.gr/
[9] F. Toshihisa and Y. Ryuichi, "Microgrid field test experiences in Japan," in *Proc. Power Eng. Soc. Gen. Meet.*, Montreal, QC, Canada, Jun. 2006.
[10] G. Celli, G. Pisano, and G. G. Soma, "Optimal participation of a microgrid to energy market with an intelligent EMS," in *Proc. Int. Power Eng. Conf.*, Nov. 2005, vol. 2, pp. 663–668.
[11] J. D. Kueck, R. H. Staunton, S. D. Labinov, and B. J. Kirby, "Microgrid energy management system," [Online]. Available: http://certs.lbl.gov/pdf/phase2-kueck.pdf
[12] F. Pilo, G. Pisano, and G. G. Soma, "Neural implementation of microgrid central controllers," in *Proc. IEEE Int. Conf. Ind. Informatics*, Jun. 2007, vol. 2, pp. 1177–1182.
[13] C. A. Hernandez-Aramburo, T. C. Green, and N. Mugniot, "Fuel consumption minimization of a microgrid," *IEEE Trans. Ind. Appl.*, vol. 41, no. 3, pp. 673–681, May/Jun. 2005.
[14] H. K. Kang, S. J. Ahn, and S. I. Moon, "A new method to determine the droop of inverter-based DGs," in *Proc. Power Eng. Soc. Gen. Meet.*, Calgary, AB, Canada, Jul. 2009.
[15] S. J. Ahn, "A new power sharing method for distributed generations in the next-generation grid," Ph.D. dissertation, Seoul National University, Seoul, Korea, Aug. 2009.
[16] [Online]. Available: http://www.epa.gov/CHP/basic/catalog.html
[17] S. J. Ahn, J. W. Park, I. Y. Chung, S. I. Moon, S. H. Kang, and S. R. Nam, "Power-sharing method of multiple distributed generators considering control modes and configurations of a microgrid," *IEEE Trans. Power Del.*, vol. 25, no. 3, pp. 2007–2016, Jul. 2010.
[18] K.-L. Nguyen, D. J. Won, S. J. Ahn, and I. Y. Chung, "Power sharing method for a grid connected microgrid with multiple distributed generators," *J. Electr. Eng. Technol.*, vol. 7, no. 4, pp. 459–467, Jul. 2012.
[19] A. Sfetsos, "A novel approach for the forecasting of mean hourly wind speed time series," *Renewable Energy*, vol. 27, pp. 163–174, 2002.
[20] G. H. Riahy and M. Abedi, "Short term wind speed forecasting for wind turbine applications using linear prediction method," *Renewable Energy*, vol. 33, pp. 35–41, 2008.
[21] A. J. Wood and B. F. Wollenberg, *Power Generation, Operation, and Control*. Hoboken, NJ, USA: Wiley, 1996.
[22] B. Rampriya, K. Mahadevan, and S. Kannan, "Application of differential evolution to dynamic economic dispatch problem with transmission losses under various bidding strategies in electricity markets," *J. Electr. Eng. Technol.*, vol. 7, no. 5, pp. 681–688, Nov. 2012.
[23] J. A. Pecas Lopes, C. L. Moreira, and A. G. Madureira, "Defining control strategies for microgrids islanded operation," *IEEE Trans. Power Syst.*, vol. 21, no. 2, pp. 916–924, May 2006.
[24] A. M. Azmy and I. Erlich, "Online optimal management of PEM fuel cell using neural networks," *IEEE Trans. Power Del.*, vol. 20, no. 2, pp. 1051–1058, Apr. 2005.
[25] M. Y. El-Sharkh, A. Rahman, and M. S. Alam, "Evolutionary programming-based methodology for economical output power from PEM fuel cell for micro-grid application," *J. Power Sources*, vol. 139, pp. 165–169, 2005.
[26] Energy Information Administration, *Natural Gas Navigator* [Online]. Available: http://tonto.eia.doe.gov/dnav/ng/ng_pri_sum_dcu_nus_m.htm
[27] C. L. Chen and N. Chen, "Direct search method for solving economic dispatch problem considering transmission capacity constraints," *IEEE Trans. Power Syst.*, vol. 16, no. 4, pp. 764–769, Nov. 2001.
[28] C. L. Chen, S. C. Hsieh, T. Y. Lee, and C. L. Lu, "Optimal integration of wind farms to isolated wind-diesel energy system," *Energy Convers. Manage.*, vol. 49, pp. 1506–1516, 2008.
[29] C. L. Chen, "Optimal generation and reserve dispatch in a multi-area competitive market using a hybrid direct search method," *Energy Convers. Manage.*, vol. 46, pp. 2856–2872, 2005.

Seon-Ju Ahn (S'04–M'09) received the B.S., M.S., and Ph.D. degrees in electrical engineering from Seoul National University, Seoul, Korea, in 2002, 2004, and 2009, respectively.

He was a Postdoctoral Researcher at Myongji University, Korea, and FREEDM System Center, NC State University, Raleigh. Currently, he is an Assistant Professor at Chonnam National University, Gwangju, Korea. His research interests are power quality, distributed energy resources, microgrids, smart grids, and real-time simulation.

Soon-Ryul Nam (S'96–M'02) received the B.S., M.S., and Ph.D. degrees in electrical engineering from Seoul National University, Seoul, Korea in 1996, 1998, and 2002, respectively.

Currently, he is an Associate Professor at Myongji University, Yongin, Korea. He was with Hoysung Corp., Seoul, from 2002 to 2005 and was a Research Professor at Myongji University, Yongin, Korea, from 2005 to 2007. He was a Postdoctoral Research Associate at Texas A&M University, College Station, and an Assistant Professor at Chonnam National University, Gwangju, Korea, from 2007 to 2009. His research interests are the protection, control, and automation of power systems.

Joon-Ho Choi (S'98–M'02) received the B.S., M.S., and Ph.D. degree in electrical engineering from Soongsil University, Seoul, Korea, in 1996, 1998, and 2002, respectively.

He was a BK21 Postdoctoral Fellow at Seoul National University. Currently, he is an associate professor at Chonnam National University, Gwang-ju, Korea. His interests include operation and integration strategies of distributed generation, distribution automation, and modeling and operation algorithms of the smart grid.

Seung-Il Moon (M'93) received the B.S. degree in electrical engineering from Seoul National University, Seoul, Korea, in 1985, and the M.S. and Ph.D. degrees in electrical engineering from Ohio State University, Columbus, in 1989 and 1993, respectively.

Currently, he is a Professor of the School of Electrical Engineering and Computer Science at Seoul National University. His special fields of interest include power quality, flexible ac transmission systems, renewable energy, distributed generation, and smart grids.